The TF Ripple Experiment

Modification of the JET Toroidal Field System

M. Huart, D. Chiron, P. Doyle, V. Marchese, G. Sannazzaro,
P. G. Smith, B. Tubbing, G. Zullo
JET Joint Undertaking, Abingdon, Oxon OX14 3EA, U.K.

ABSTRACT

The interleaved structure of the TF coils allows to obtain a programmable TF ripple field by feeding the two sub-sets of the TF coils with different currents. This would allow to vary the ripple field within one JET pulse and allow a direct assessment of the increased ripple on confinement time, fast particle losses, plasma rotation and H-mode. The TF ripple experiment (RIPPLE 2) was carried out in the Pumped Divertor configuration in conditions relevant to ITER. In this configuration, the normal field ripple at the plasma edge is about 0.1%. In the experiment, the ripple field was varied up to 2% at the plasma edge, the plasma current was typically 2-3MA and the TF field 2-2.5T.

I. INTRODUCTION

The JET Toroidal Field Power Supplies [1] comprise of a flywheel generator with two series connected diode rectifiers (TFGC) and two mains driven transformer-thyristor rectifiers (TF-SU1/TF-SU2) symmetrically arranged. The mid-point of the TFGC diode rectifiers is grounded via a high impedance resistor.

The JET Toroidal Field Coils (fig. 1) comprise of two sub-sets of 16 coils, interleaved with upper and lower terminals, with two compensating busbars for the upper and lower terminal connections.

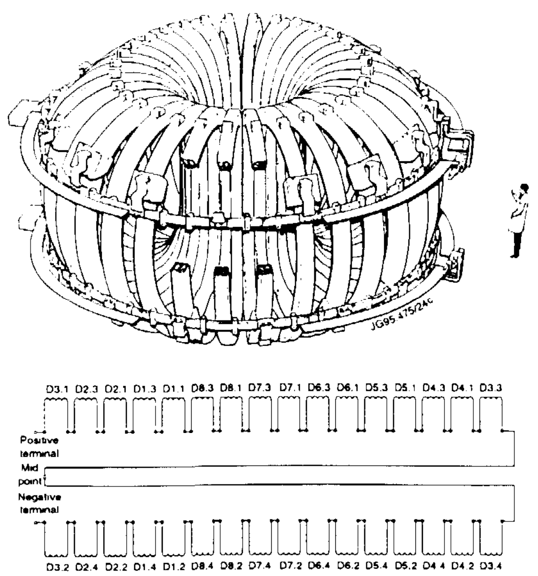

Fig 1. 3D Overview and electrical schematic diagram of the JET 32 TF coils.

II. NEW TF CIRCUIT CONFIGURATION

The Toroidal Field Coil System was designed with a mid-point busbar with current carrying capability for the operation with 16 coils (fig 1.). Whereas the TFGC diode convertors have indeed a mid-point (fig. 2a), a differential current cannot be maintained in the two stator windings since it will produce an overheating of the rotor damper cage. Therefore, the Toroidal Field Power Supplies need to be re-arranged in an asymmetric configuration (fig. 2b) with a new neutral busbar designed to carry the rated imbalance current (table 1). The change of configuration is achieved by new busbars and bolted links.

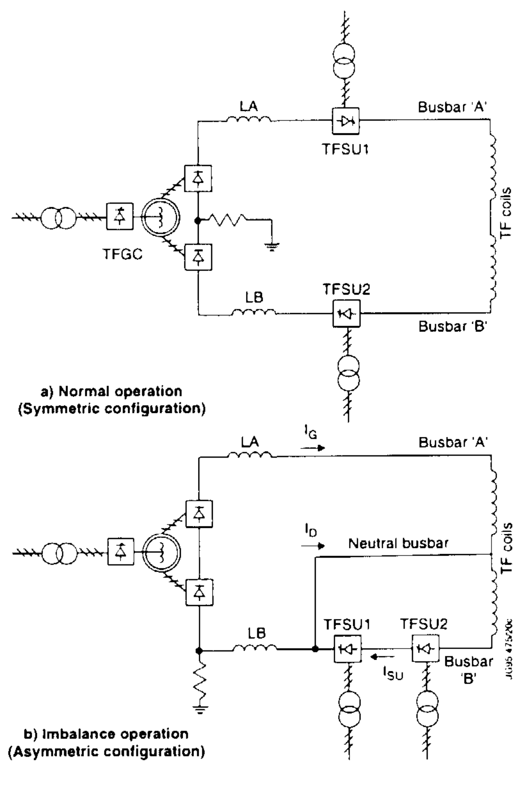

Fig 2. Configuration of the TF Power Supplies

TABLE 1 - SCENARIO OF RIPPLE 2 EXPERIMENT

SCENARIO NO. 1:		SCENARIO NO. 2:	
Toroidal Field	: 2.5T	Toroidal Field :	2.0T
Average TF current	: 50kA	Average TF current:	40kA
Imbalance TF current:	30kA	Imbalance TF current :	40kA
TF Ripple δ	: 0.3 x δ_{16}	TF Ripple δ :	0.5 x δ_{16}
Maximum duration of the imbalance current: 10s			

III. FAULT ANALYSIS - CONTROL FAULTS

In the imbalance configuration of the TF circuit (fig 2b), the two sets of 16 TF coils are supplied from different power supplies. In view of the strong coupling between the two sub-sets of coils (interleaved structure) a fault involving the freewheeling of one power supply will lead to a rapid increase of the current in the "healthy" loop (up to twice the average current). Control faults can therefore be severe and needed proper analysis. Three fault scenarios were identified, all three occurring at the end of the TF current rise (TFGC output voltage is highest):

scenario no. 1: the TF-SU1/TF-SU2 output voltages go to zero (freewheeling). The negative imbalance current is detected and trip the flywheel generator (normal operation, $I_D \geq 0$)

scenario no. 2: as scenario no. 1, but the protection fails. When the current detected by the TFC-DCCT exceeds 55kA, the flywheel generator is tripped on DC overcurrent (fig 3).

scenario no. 3: the FGC-DCCT fails (output to zero). The control loops react by exciting the TFGC and de-exciting the TF-SU's. When the current, detected by the FGC ACCT's, exceeds 70kA (DC equivalent), the flywheel generator is tripped on AC overcurrent.

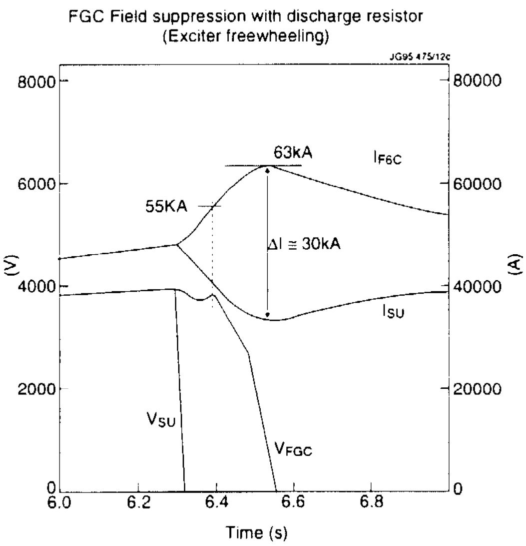

Fig. 3 Fault Scenario no. 2: loss of TF-SU1/TF-SU2 (freewheeling) during TF current rise

IV. OVERVIEW OF CONTROL AND PROTECTION SYSTEM

A. *Control System*

In the Ripple-2 Experiment, the TF currents are best defined by two variables, namely the TF coil average current (I_{AV}) and the TF coil imbalance current (I_D). The average current defines the magnetic field on axis (B_T) while the imbalance current defines the ripple (δ) defined as amplitude of the field perturbation.

We have $\frac{\delta}{\delta_{16}} = \frac{I_D}{2 I_{AV}}$ $(0 < \frac{\delta}{\delta 16} < 0.5)$, δ_{16} = pure 16 coils

In view of the different time response of the power supplies and the different time constant of the circuits (table 2), the control system was designed as two separate control loops (fig. 4); the TF average current loop controls the TFGC and the TF imbalance current loop controls the TF-SU1/TF-SU2.

TABLE 2 - CIRCUIT CHARACTERISTICS

1. MAIN CIRCUIT (AVERAGE CURRENT)	2. IMBALANCE CIRCUIT (IMBALANCE CURRENT)
- INDUCTANCE : 660mH	- INDUCTANCE (CALC.) : 9.5mH
- RESISTANCE : 62 mΩ	- RESISTANCE:: 16.5 mΩ
- TITLE CONSTANT: 10.6S	- TIME CONSTANT: 0.6s

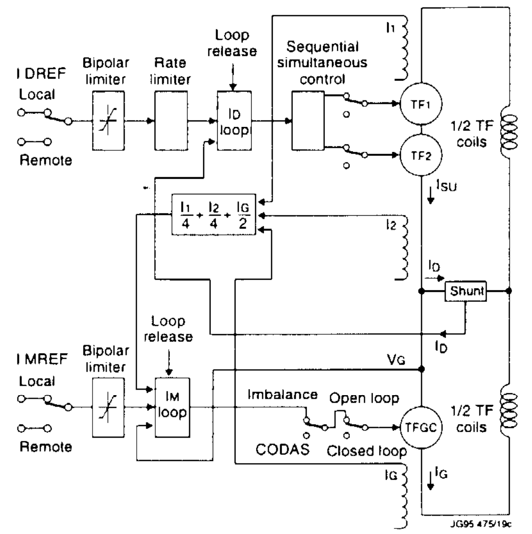

Fig. 4 Control loops for TF average current and imbalance

B. *Protection System*

B.1. TF Load Interface Cubicle. Control faults can have severe consequences. Hence the need to integrate the control and associated detection/protection system into one single equipment. The TF Load Interface Cubicle was designed for this purpose.

The hardwired protection logic (fig. 5) is designed to coordinate the protection actions between the three power supplies, TFGC, TF-SU1 and TF-SU2. Three levels of protection actions are foreseen (action levels).

B2. Coil Protection System (CPS) The TF measurements for the coil protection system was changed to be consistent with the new circuit configuration. Likewise, the settings of overcurrent trips were set as I1A = 55kA (+5%, + 10%) and I1B = 65kA (+5%, +10%). In addition, the model of the TF circuit, built-in within CPS, was changed from a

one circuit to two circuits equation. This model computes coil voltages from measured currents and compares with the measured voltages and trips once a discrepancy is detected.
Most faults have two detection levels corresponding to the protection action level 2 and 3.

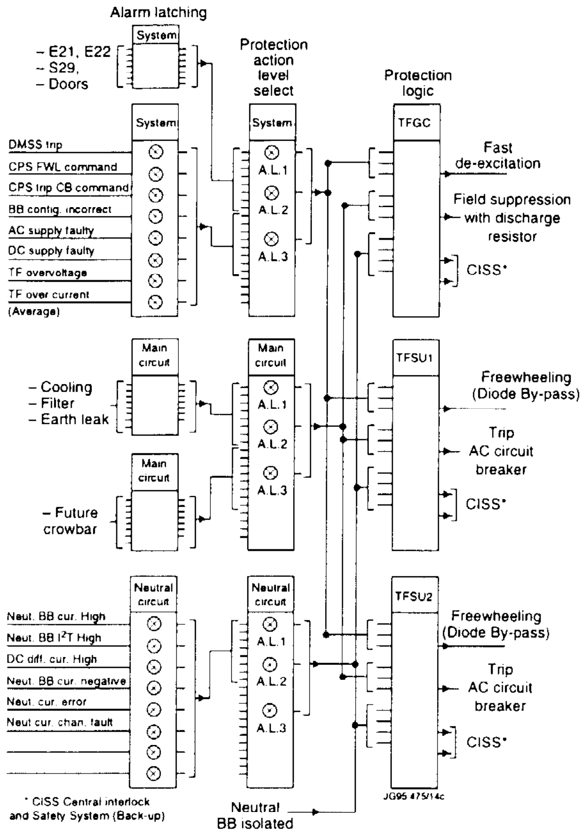

Fig. 5 Hardwired Protection Logic

V. ANALYSIS OF STRESSES IN THE TOROIDAL FIELD COILS

A. Operation With Imbalance Current

A.1. In-plane loads. The stresses in the TF coils were calculated for the two scenarios defined in table 1. Fig. 7 and 8 show the operating points of scenarios no. 1 and 2, respectively axial stress and shear stress, due to in-plane loads only. They are compared with the operating points corresponding to normal operation at 3.45T and to the operation with 16 coils only (Ripple-1 experiment).
From fig. 7 and 8, it is clear that scenario no. 1 has higher axial and shear stress than scenario no. 2.
A2. In-plane and out-of-plane loads. The total axial and shear stress was calculated for scenario no. 1. The maximum values obtained are:

- axial stress (copper) : 66 MPA (<100 MPa)
- shear stress (insulation) : 9.5 MPa (<15MPa)

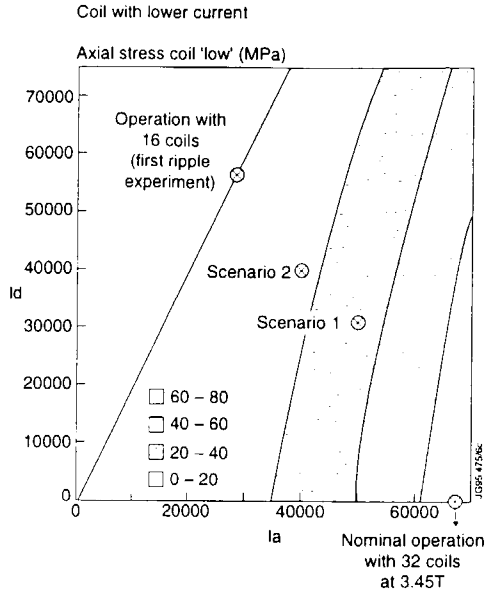

Fig. 7 Axial Stress in TF Coils with variable imbalance current (in-plane loads only)

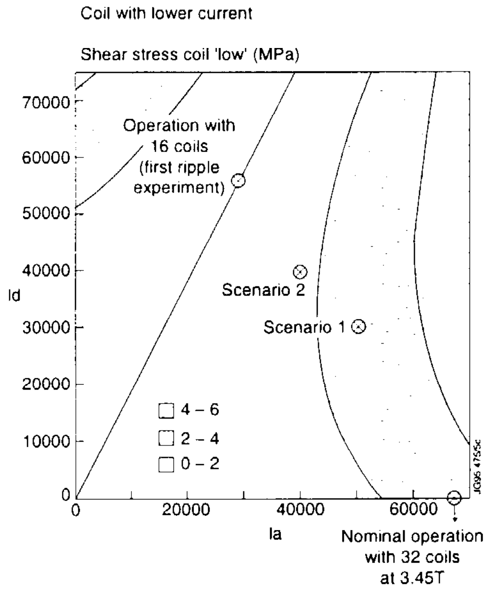

Fig. 8 Shear stress in TF coils with variable imblance current (in - plane loads only)

B. Fault Scenarios

Table 3 summarises the maximum fault currents calculated in the three faults scenario no. 1, 2, 3 (see III above) and for three cases of FGC trips, namely:

a. full inversion of FGC exciter (field inversion)
b. freewheeling of FGC exciter and insertion of discharge resistor in excitation circuit (field suppression)
c. failure of exciter to freewheel followed 100ms later by insertion of discharge resistor.

TABLE 3 - FAULT CURRENTS

Fault Scenario	1a	2a	2b	2c	3b	3c
TFGC Peak Current (kA)	57	59	63	69	76	80
Imbalance Peak Current (kA)	-20	-25	-30	-42	-57	-63

Table 4 summarises the maximum stresses. It should be noted that, as a result of the simulation of the control faults (reported in III above), the following measures were implemented:

a. measurements of the imbalance current (with current shunt) instead of computation from the difference of the FGC/TFSU currents
b. detection of negative imbalance current and trip set at -5kA
c. detection of error $e = I_{SU} - I_{FGC} - I_D$ (imbalance current error) and trip set at 5kA absolute
d. detection of error $e = I_{DREF} - I_D$ (imbalance current error) and trip set at 10kA absolute.

TABLE 4 - MAXIMUM STRESSES IN FAULT CONDITIONS

FAULT SCENARIO	INTERTURN SHEAR STRESS (MPa)	TENSILE STRESS IN COPPER (MPa)
2c	10	85
3b	12	106
3c	13	121

To obtain the fault currents calculated in scenario no. 3 would require the simultaneous failures of protections b,c and d above.

VI. EXPERIMENTAL RESULTS

A. Power Commissioning

The power commissioning included live tests of the protection system during the TF current rise phase. These tripping tests allowed to verify the simulations results reported under III above. The experimental results show that the peak value of the imbalance current is larger than expected, even after correction of the simulation to take account of the actual FGC speed.

Good corrolation of experimental and simulated results were obtained by increasing the mutual inductance from 153 mH to 156 mH. The inductance of the imbalance circuit (table 2) is correspondingly reduced from 9.5mH to 8.0mH.

These new values were used to update the fault currents given in table 3. These are shown in table 5 (old values shown in bracket).

TABLE 5 - FAULT CURRENTS (WITH CORRECTED COEFFICIENTS)

Fault Scenario	2a	2b	2c	3b
TFGC Peak Current (kA)	62 (59)	66.5 (63)	71 (69)	80 (76)
Imbalance Peak Current (kA)	-29 (-25)	-37 (-30)	-45 (-42)	-64 (-57)

B. Ripple-2 Experiment

The Ripple - 2 Experiment was carried out with JET in the Pumped Divertor Configuration. In this configuration, the edge ripple (δ_{32}) is about 0.1%. The toroidal field circuit was operated with a variable imbalance current to produce a N = 16 ripple component. The edge ripple was varied up to 0.5 x δ_{16} (equivalent to about 2%).

With NBI injection, loss of plasma energy of the order of about 5% were measured while the plasma rotation was reduced by a factor 2 with a 1% ripple. These losses appear somewhat larger than expected on the basis of classical theory.

The ripple field had some peculiar effects on the H-mode. While with a ripple field of 1% a small improvement in H-mode performance is obtained (elm behavior), a degradation of the H-mode performance was observed with a ripple field of 2%. The H-mode threshold is somewhat lowered in the presence of a ripple field (fig 9).

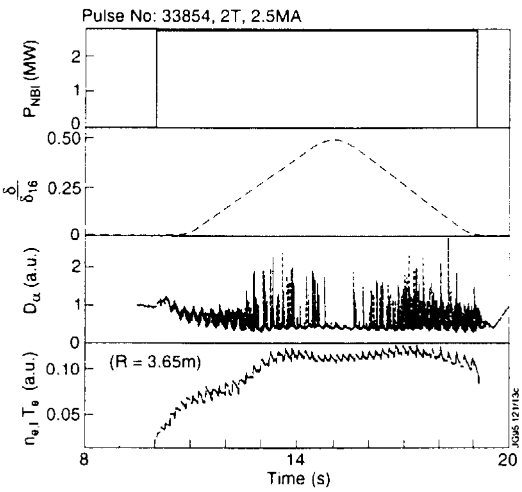

Fig. 9 Effect of varying ripple on H-mode, with PNIB near the threshold.

ACKNOWLEDGEMENT

The authors wish to thank the Chief Engineer, Dr. E Bertolini, for his leadership in coordinating the studies on the fault scenarios in this new configuration of the TF circuit.

REFERENCES

[1] E. Bertolini et al, *"The JET Magnet Power Supplies and Plasma Control System"*, Fusion Technology, Volume 11, Number 1, pp71-119.

[2] B J D Tubbings et al, *"Experiments with Toroidal Field Ripple in JET"*, Proceedings of the 22nd EPS Conference on Control Fusion and Plasma Physics, Bournemouth (UK), July 1995 (to be published).